International Journal of the Korean Society of Precision Engineering, Vol. 1, No. 1, June 2000.

Analysis of 3-D Cutting Process with Single Point Tool

Young Moon Lee*, Won Sik Choi ** and Tae Seong Song ***

*Department of Mechanical Engineering, Kyungpook National University, Taegu, South Korea
**Department of Mechanical Engineering, Miryang National University, Miryang, South Korea
***Graduate School, Kyungpook National University, Taegu, South Korea

ABSTRACT

This study presents a procedure for analyzing chip-tool friction and shear processes in 3-D cutting with a single point tool. The edge of a single point tool including a circular nose is modified to an equivalent straight edge, thereby reducing the 3-D cutting with a single point tool to the equivalent of oblique cutting. Then, by transforming the conventional coordinate systems and using the measurements of three cutting force components, the force components on the rake face and shear plane of the equivalent oblique cutting system can be obtained. As a result, the chip-tool friction and shear characteristics of 3-D cutting with a single point tool can be assessed.

Key Words: Single point tool, oblique cutting, inclination angle (i), side cutting edge angle (C_s), chip flow angle (η_c), specific friction energy (u_f), specifie shear energy (u_s), specific cutting energy (u)

1. Introduction

In metal cutting process, a chip is produced by concentrated shear processes occurring at very short intervals within the extremely limited region of the shear zone or primary shear zone. The produced chip then experiences severe friction with the tool rake face before being externally discharged. As a result, the chip that is formed is located between the shearing region and the chip-tool frictional region. The shear process can be characterized by various cutting variables including the shear strain, shear stress and shear velocity, whereas the friction process can be characterized by the friction force, friction coefficient and, chip velocity.

However, these variables have an effect on one another and cannot be considered independently[1].

Therefore, the fundamental issue for research related to metal cutting is to identify the effects of the cutting conditions on the shear and friction processes plus the interrelationship between these two processes.

Cutting processes can be classified into two-dimensional cutting, which refers to orthogonal cutting, and 3-D cutting based on the geometrical and kinematical relationships of the tool and the workpiece.

Until now, most metal cutting studies have concentrated on the orthogonal cutting process as it is easier to analyze and identify the mutual relations among the cutting variables compared with the 3-D processes.

However, in practice, most cutting processes are 3-D and the deformation of a workpiece during chip formation is three dimensional, which makes the analysis very difficult.

The first study on 3-D cutting focused on oblique cutting, which is the simplest 3-D cutting process. Merchant[2] established the force and velocity relations in oblique cutting. Shaw et al[3] analyzed the shear and frictional characteristics in oblique cutting. Zorev[4] analyzed the chip formation mechanism and force balance in 3-D cutting with a single point tool with two straight edges. Usui and his colleagues[5] tried to estimate the cutting force components of 3-D cutting with a single point tool with two straight edges using two-dimensional cutting data.

However, in practice, most single point tools have a circular nose which connects two straight edges.

Accordingly, this study presents a procedure for analyzing the chip-tool friction on the tool rake face along with the shear process in the primary shear zone in 3-D cutting with a single point tool that has a circular nose.

2. Three Dimensional Cutting

2.1 Inclination angle, i

Orthogonal cutting is defined as cutting in which the straight cutting edge stays orthogonal with a cutting velocity vector, as seen in Fig. 1(a).

If the position of the cutting edge deviates from this then the cutting becomes three-dimensional. The simplest three-dimensional cutting is oblique cutting in which a straight cutting edge is inclined to the velocity vector as seen in Fig.1(b) and 1(c).

The inclination angle, i is the distinguishing feature between 3-D and 2-D cutting.

In this study, for an appropriate analysis of the cutting dynamics, the signs of the inclination angle are designated according to the established axis.

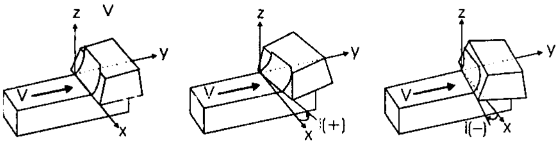

Fig. 1 Comparison of orthogonal (a), and oblique (b), (c) cutting operation

2.2 Equivalent oblique cutting

In this study, an equivalent oblique cutting model to a 3-D cutting process with a single point tool was created to analyze the friction between the chip and the tool rake face and the shear process on shear plane.

Fig. 2 illustrates the most practical cutting process performed by a single point tool, turning.

Here the primary cutting edge is the side cutting edge connected by a circular nose to the secondary edge. To obtain an equivalent oblique cutting system to this it is necessary to replace the active side cutting edge with a circular nose as an equivalent straight edge, i.e. an equivalent side cutting edge.

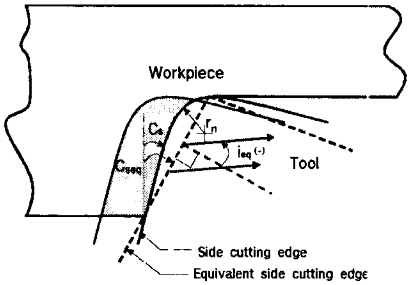

Fig. 2 Definition of C_{seq} on tool face

Lee et al[6] presented a method to determine the equivalent side cutting edge angle C_{seq}.

If the angle C_{seq}, the side rake angle α_s and the back rake angle α_b are given, the equivalent inclination angle i_{eq} and the equivalent velocity rake angle α_{veq} can be found as follows[7]:

$$\tan i_{eq} = \tan\alpha_b \cos C_{seq} - \tan\alpha_s \sin C_{seq} \tag{1}$$

$$\tan\alpha_{veq} = \tan\alpha_s \cos C_{seq} + \tan\alpha_b \sin C_{seq} \tag{2}$$

Using eqn.(1) and (2) with the given chip flow angle η_c, the angles of the equivalent oblique cutting system can be expressed as follows:

$$\tan\alpha_{neq} = \cos i_{eq} \tan\alpha_{veq} \tag{3}$$

$$\sin\alpha_{eeq} = \sin\eta_c \sin i_{eq} + \cos\eta_c \cos i_{eq} \sin\alpha_{neq} \tag{4}$$

$$\tan\phi_{neq} = \frac{t/t_c \cos\alpha_{neq}}{1 - t/t_c \sin\alpha_{neq}} \tag{5}$$

$$\tan\eta_s = \frac{\tan i_{eq}\cos(\phi_{neq} - \alpha_{neq}) - \tan\eta_c \sin\phi_{neq}}{\cos\alpha_{neq}} \tag{6}$$

$$\sin\phi_{eeq} = \frac{\cos\eta_s \cos\alpha_{eeq}}{\cos\eta_c \cos\alpha_{neq}}\sin\phi_{neq} \tag{7}$$

Here, α_{neq}, α_{eeq}, ϕ_{neq}, η_s and ϕ_{eeq} are the equivalent normal rake, effective rake, normal shear, shear flow, and effective shear angle, respectively.

3. Analysis of cutting forces

3.1 Cutting force components applied on tool rake face

In turning, there are three components of the cutting force. In a right-hand coordinate system they are the radial component F_x, the vertical component F_y and the axial component F_z, as shawn in Fig. 3.

In order to evaluate a three-dimensional cutting proecss, it is necessary to determine three mutually perpendicular force components.

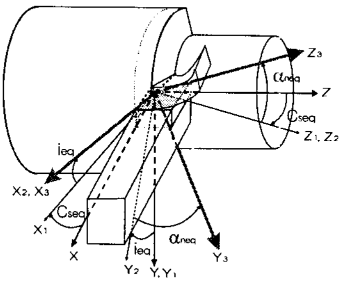

(a)

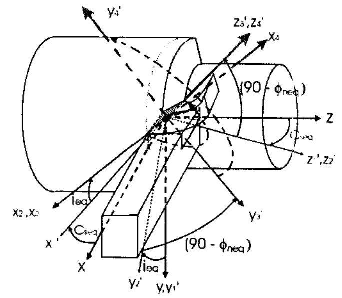

(b)

Fig. 3 Coordinate system in turning: (a) On rake face and (b) On shear plane

These force components can be measured during cutting using a three component tool dynamometer.

To identify the force components in the plane of the tool rake face, it is convenient to change to the $x_3y_3z_3$ right-hand coordinate system as seen in Fig.3(a) where x_3 is along the equivalent side cutting edge, y_3 is normal to the tool rake face, and z_3 is normal to the equivalent side cutting edge yet in the plane of the tool rake face.

Eqn.(8) represents this transformation.

$$\begin{bmatrix} F_{Rx} \\ F_{Ry} \\ F_{Rz} \end{bmatrix} = \begin{bmatrix} 1 & 0 & 0 \\ 0 & \cos\alpha_{neq} & -\sin\alpha_{neq} \\ 0 & \sin\alpha_{neq} & \cos\alpha_{neq} \end{bmatrix} \begin{bmatrix} \cos i_{eq} & \sin i_{eq} & 0 \\ -\sin i_{eq} & \cos i_{eq} & 0 \\ 0 & 0 & 1 \end{bmatrix} \times \begin{bmatrix} \cos C_{seq} & 0 & -\sin C_{seq} \\ 0 & 1 & 0 \\ \sin C_{seq} & 0 & \cos C_{seq} \end{bmatrix} \begin{bmatrix} F_x \\ F_y \\ F_z \end{bmatrix} \tag{8}$$

The friction coefficient μ is defined as the tangential force devided by the normal force. Providing the angle ρ_c is the angle between the direction of the resultant tangential force on the tool rake face and the chip flow direction, μ can be expressed as eqn.(9).

$$\mu = \frac{[F^2_{Rx} + F^2_{Rz}]^{1/2} \cos\rho_c}{F_{Ry}} \tag{9}$$

3.2 Cutting force components in shear plane

To identify the force components in the shear plane, it is also convenient to change the given xyz to the $x_4' y_4' z_4'$ right-hand coordinate system as seen in Fig. 3(b) where x_4' is also along the equivalent side cutting edge, y_4' is normal to the shear plane, and z_4' is normal to the equivalent side cutting edge yet in the shear plane.

Eqn.(10) represents this transformation

$$\begin{bmatrix} F_{Sx} \\ F_{Sy} \\ F_{Sz} \end{bmatrix} = \begin{bmatrix} \cos 180 & \sin 180 & 0 \\ -\sin 180 & \cos 180 & 0 \\ 0 & 0 & 1 \end{bmatrix} \begin{bmatrix} 1 & 0 & 0 \\ 0 & \cos(90-\phi_{neq}) & \sin(90-\phi_{neq}) \\ 0 & -\sin(90-\phi_{neq}) & \cos(90-\phi_{neq}) \end{bmatrix} \times \begin{bmatrix} \cos i_{eq} & \sin i_{eq} & 0 \\ -\sin i_{eq} & \cos i_{eq} & 0 \\ 0 & 0 & 1 \end{bmatrix} \begin{bmatrix} \cos C_{seq} & 0 & -\sin C_{seq} \\ 0 & 1 & 0 \\ \sin C_{seq} & 0 & \cos C_{seq} \end{bmatrix} \begin{bmatrix} -F_x \\ -F_y \\ -F_z \end{bmatrix} \tag{10}$$

Providing the angle ρ_s is the angle between the resultant force in the shear plane and the shear flow direction, then the shear stress τ and the shear strain γ can be expressed as follows:

$$\tau = \frac{F_s}{fd} \sin\phi_{neq} \cos i_{eq} \cos\rho_s \tag{11}$$

$$\gamma = \frac{\cot\phi_{neq} + \tan(\phi_{neq} - \alpha_{neq})}{\cos\eta_s} \tag{12}$$

3.3 Cutting energy

Practically all the energy associated with a cutting operation is consumed in either plastic deformation or friction [8].

3.3.1. Specific friction energy u_f

The specific friction energy u_f is defined as the friction energy per unit time divided by the volume removed per unit time, as seen in eqn.(13).

$$u_f = \frac{[F^2_{Rx} + F^2_{Rz}]^{1/2} \cos\rho_c V_c}{fdV} \tag{13}$$

where V_c is the chip velocity and V is the cutting velocity, and between them the following relation should be satisfied.

$$\frac{V_c}{V}=\frac{\cos i_{eq}\sin\phi_{neq}}{\cos\eta_c\cos(\phi_{neq}-\alpha_{neq})} \qquad (14)$$

If eqn.(14) is simplified by the use of Stabler's chip flow rule[9], then eqn.(13) can be expressed as fllows:

$$u_f=\frac{[F^2_{Rx}+F^2_{Rz}]^{1/2}\cos\rho_c\sin\phi_{neq}}{fd\cos(\phi_{neq}-\alpha_{neq})} \qquad (15)$$

3.3.2 Specific shear energy, u_s

The specific shear energy can be similarly found as seen in eqn.(16).

$$u_s=\frac{[F^2_{Sx}+F^2_{Sz}]^{1/2}\cos\rho_s V_s}{fdV} \qquad (16)$$

where V_s is the shear velocity and V is the cutting velocity, and between them the following relation should be satisfied.

$$\frac{V_s}{V}=\frac{\cos i_{eq}\cos\alpha_{neq}}{\cos\eta_s\cos(\phi_{neq}-\alpha_{neq})} \qquad (17)$$

From eqn.(16) and (17) u_s can be expressed as follows:

$$u_s=\frac{[F^2_{Sx}+F^2_{Sz}]^{1/2}\cos\rho_s\cos i_{eq}\cos\alpha_{neq}}{fd\cos\eta_s\cos(\phi_{neq}-\alpha_{neq})} \qquad (18)$$

3.3.3 Specific cutting energy u

The specific cutting energy u is defined as the cutting energy per unit time divided by the volume removed per unit time as seen in eqn.(19).

$$u=\frac{F_y}{fd} \qquad (19)$$

where F_y is the main cutting force component, f is the feed rate, and d is the depth of cut.

4. Experiments

A series of cutting experiments on commercially available steel workpieces were performed to verify the validity of the proposed procedure for analyzing chip-tool friction and shear processes.

Two kinds of hot rolled steels (SM45C and SS41) were turned.

Table 1 shows the chemical compositions of the workpieces.

Table 1 Chemical composition(wt%) of SM45C and SS41 steels

	C	Si	Mn	P	S
SM45C	0.427	0.218	0.679	0.011	0.010
SS41	0.160	0.210	0.562	0.013	0.015

Cutting tests were run for each workpiece with varying feed rates and cutting velocities, a constant cutting depth, and without a coolant.

Table 2 Cutting input conditions

Cutting Speed	: 100 m/min, 200 m/min
Depth of cut	: 2 mm
Feed rate	: 0.067, 0.148, 0.234, 296, 0.345, 0.444, 0.542, 0.641 (mm/min)
Insert	: TNMG 160408 (KT 350)
Nose radius	:0.8 mm
Side cutting edge angle	: -1 °
Back rake angle	: -6 °
Side rake angle	: -6 °
Tool holder	: PTGNL2525M16
Cutting Fluid	: None

Table 2 shows the input conditions including the tool inserts used of the cutting tests.

The three cutting force components were measured using a piezo-type dynamometer and the force signals were digitized and stored using a microprocessor-controlled data acquisition system.

5. Experimental results and discussions

As mentioned earlier, no previous attempt has been made to analyze frictional and shear characteristics seperately in a 3-D cutting operation, except for in oblique cutting. Therefore, until now, one of the most commonly used methods for assessing a 3-D cutting operation is based on the specific cutting energy consumed[11].

As shown in eqn.(19), the specific cutting energy is the cutting energy consumed per unit volume of material removed.

Fig. 4 shows the specific cutting energy results. With an increase in the feed rate the specific cutting energy consumed decreased. This could be explained by the 'size effect' during cutting[10].

Also shown in the same figure, SS41 steel consumed less energy than SM45C steel. This variance may be related to the different carbon content in the two steels.

Plus, under higher cutting speed conditions (200m/min), the amount of energy consumed was lower.

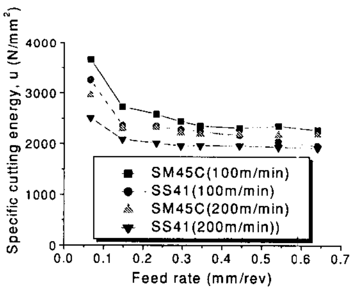

Fig. 4 Specific cutting energy u vs. feedrate (mm/rev)

Fig. 5 and 6 show the specific friction energy and specific shear energy obtained according to eqn.(15) and (18), respectively.

There was no significant difference in the specific friction energy between SM45C and SS41 steel.

And it tended to decrease with an increase in the feed rate. This may be partly explained by the 'size effect' during cutting.

Another reason may be the fact that as the feed rate increased, angle between the resultant force on the tool rake face and the chip flow direction increased, thereby causing a decrease in the active friction force component leading to a reduction in the friction energy.

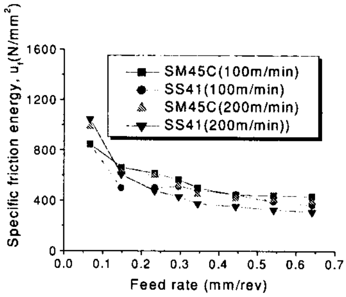

Fig. 5 Specific friction energy u_f vs. feedrate (mm/rev)

As with the specific cutting energy, under higher cutting speed conditions, the friction energy consumed was lower. In general, as the cutting speed increases the chip-tool contact length decreases and this causes a reduction in the friction energy[12].

As can be seen in Fig. 6, the specific shear energy tended to decrease in a low feed rate region and yet became constant as the feed rate increased, except when cutting SS41 steel under 200m/min cutting speed conditions.

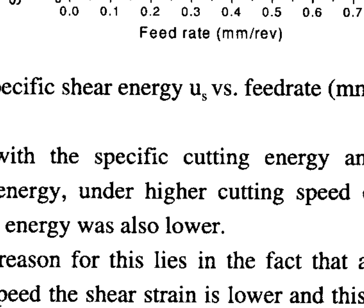

Fig. 6 Specific shear energy u_s vs. feedrate (mm/rev)

As with the specific cutting energy and specific friction energy, under higher cutting speed conditions, the shear energy was also lower.

The reason for this lies in the fact that at a higher cutting speed the shear strain is lower and this leads to a reduction in the shear energy consumed.

As shown in the appendix, since all the energy is consumed in either plastic deformation or friction, the sum of the specific shear energy u_s and the specific friction energy u_f should be equal to the specific cutting energy u.

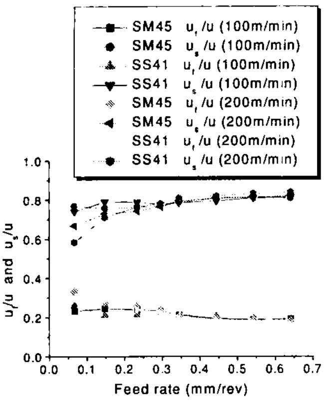

Fig. 7 Ratio of specific friction energy to specific cutting energy u_f/u and specific shear energy to specific cutting energy u_s/u vs. feedrate (mm/rev)

Fig. 7 represents the ratios of the specific shear energy u_s and the specific friction energy u_f to the specific cutting energy u.

As seen in this figure, the shear energy accounts for about 60-80 percent of the total energy, while 20-40 percent is due to friction.

These results mached well with the results from orthogonal and oblique cutting[13],[3].

6. Conclusions

This paper introduced an equivalent oblique cutting system for analyzing the friction between a chip and the tool rake face and the shear in the primary shear zone in 3-D cutting with a single point tool.

Analytical relationships were established for the friction and shear force components in a turning operation in terms of three cutting force components determined using a tool dynamometer.

In addition, it was confirmed that all the energy was consumed in the friction and shear processes.

To verify the validity of the proposed procedure for analyzing friction and shear processes in 3-D cutting with a single point tool, a series of cutting tests were performed.

The experimental results on the friction and shear characteristics matched well with previous results obtained from orthogonal and oblique cutting tests.

Reference

1. N.N. Zorev, "Interrelationship Between Shear Processes Occurring Along Tool Face and on Shear Plane in Metal Cutting," Pro. Inter. Res. Prod. Conf., Carnegie Inst. Of Tech., pp. 42-49, 1963.
2. M. E. Merchant, "Basic Mechanics of the Metal-Cutting Process," Journal of Applied Mechanics, TRANS. ASME, Vol. 66, pp. A-168-175, 1944.
3. M. C. Shaw, N. H. Cook, and P. A. Smith, "The Mechanics of Three Dimensional Cutting Operation," TRANS. ASME, Vol. 74, pp. 1055-1064, 1952.
4. N. N. Zorev, "Metal Cutting Mechanics," Pergamon Press, Oxford, pp. 348-377, 1966.
5. E. Usui, A. Hirota, and M. Masuko, "Analytical Prediction of Three Dimensional Cutting Process," Journal of Engineering for Industry, TRANS. ASME, Vol. 100, pp.222-228, 1978.
6. Y. M. Lee, S. J. Choi and T. J. Woo, "Analysis of the Chip Shape in Turning(I): Analysis of the Chip Flow Angle," TRANS. KSME (in korean), Vol. 15/1, pp. 139-144, 1991.
7. M. C. Shaw, "Metal Cutting Principles," Oxford Univ. Press, New York, pp. 428-450, 1984.
8. M.C. Shaw, "Metal Cutting Principles," Oxford Univ. Press, New York, pp. 30-36,1984.
9. G. V. Stabler, "The Chip Flow Law and Its Consequences," Pro. 5th. Int. Mach. Tool Des. Res. Conf.,Birmingham, pp. 243-251, 1964.
10. M.C. Shaw, and I. Finnie, "The Shear Stress in Metal Cutting," TRANS. ASME, Vol. 77, pp. 115-125, 1955.
11. I. S. Jawahir, N. Qureshi, and J. A. Arsecularatne, "On the Interrelationships of some Machinability Parameters in Finish Turning with Cermet Chip Forming Tool Inserts," Int. J. Mach Tools Manufact. Vol. 32/5, pp. 709-723, 1992.
12. E. M. Trent, "Metal Cutting," Butterworths, pp. 31-48, 1977.
13. M. E. Merchant, "Mechanics of th Metal Cutting

Process. I. Orthogonal Cutting and a Type 2 Chip," Journal of Applied Physics, Vol. 16, pp. 267-275, 1945.

Appendix

According to eqn.(15) and (18), spcific friction energy u_f and specific shear energy u_s can be expressed as follows

$$\mathbf{u_f} = \frac{[F^2{}_{Rx} + F^2{}_{Rz}]^{1/2}\cos\rho_c \sin\phi_{neq}\cos i_{eq}}{fd\cos(\phi_{neq}-\alpha_{neq})\cos\eta_c}$$

where, $\rho_c = \eta_c - \delta_c$

$$\tan\delta_c = \frac{F_{Rx}}{F_{Rz}}$$

$$\cos i_{eq} = \cos\eta_c$$

$$\begin{bmatrix} F_{Rx} \\ F_{Ry} \\ F_{Rz} \end{bmatrix} = \begin{bmatrix} 1 & 0 & 0 \\ 0 & \cos\alpha_{neq} & -\sin\alpha_{neq} \\ 0 & \sin\alpha_{neq} & \cos\alpha_{neq} \end{bmatrix} \begin{bmatrix} \cos i_{eq} & \sin i_{eq} & 0 \\ -\sin i_{eq} & \cos i_{eq} & 0 \\ 0 & 0 & 1 \end{bmatrix} \times \begin{bmatrix} \cos C_{seq} & 0 & -\sin C_{seq} \\ 0 & 1 & 0 \\ \sin C_{seq} & 0 & \cos C_{seq} \end{bmatrix} \begin{bmatrix} F_x \\ F_y \\ F_z \end{bmatrix}$$

$$\mathbf{u_s} = \frac{[F^2{}_{Sx} + F^2{}_{Sz}]^{1/2}\cos\rho_s \cos\alpha_{neq}\cos i_{eq}}{fd\cos(\phi_{neq}-\alpha_{neq})\cos\eta_s}$$

where, $\rho_s = \eta_s - \delta_s$

$$\tan\delta_s = \frac{F_{Sx}}{F_{Sz}}$$

$$\tan\eta_s = \frac{\tan i_{eq}\cos(\phi_{neq}-\alpha_{neq}) - \tan\eta_c \sin\phi_{neq}}{\cos\alpha_{neq}}$$

$$\begin{bmatrix} F_{Sx} \\ F_{Sy} \\ F_{Sz} \end{bmatrix} = \begin{bmatrix} \cos 180 & \sin 180 & 0 \\ -\sin 180 & \cos 180 & 0 \\ 0 & 0 & 1 \end{bmatrix} \begin{bmatrix} 1 & 0 & 0 \\ 0 & \cos(90-\phi_{neq}) & \sin(90-\phi_{neq}) \\ 0 & -\sin(90-\phi_{neq}) & \cos(90-\phi_{neq}) \end{bmatrix}$$

$$\times \begin{bmatrix} \cos i_{eq} & \sin i_{eq} & 0 \\ -\sin i_{eq} & \cos i_{eq} & 0 \\ 0 & 0 & 1 \end{bmatrix} \begin{bmatrix} \cos C_{seq} & 0 & -\sin C_{seq} \\ 0 & 1 & 0 \\ \sin C_{seq} & 0 & \cos C_{seq} \end{bmatrix} \begin{bmatrix} -F_x \\ -F_y \\ -F_z \end{bmatrix}$$

$$= \begin{bmatrix} -1 & 0 & 0 \\ 0 & -1 & 0 \\ 0 & 0 & 1 \end{bmatrix} \begin{bmatrix} 1 & 0 & 0 \\ 0 & \cos(90-\phi_{neq}) & \sin(90-\phi_{neq}) \\ 0 & -\sin(90-\phi_{neq}) & \cos(90-\phi_{neq}) \end{bmatrix}$$

$$\times \begin{bmatrix} \cos i_{eq} & \sin i_{eq} & 0 \\ -\sin i_{eq} & \cos i_{eq} & 0 \\ 0 & 0 & 1 \end{bmatrix} \begin{bmatrix} \cos C_{seq} & 0 & -\sin C_{seq} \\ 0 & 1 & 0 \\ \sin C_{seq} & 0 & \cos C_{seq} \end{bmatrix} \begin{bmatrix} -F_x \\ -F_y \\ -F_z \end{bmatrix}$$

Using these, $\mathbf{u_f}+\mathbf{u_s}$ can be rewriten as follows

$\mathbf{u_f}+\mathbf{u_s}=$

$$\left(\begin{aligned} & F_x \times \{-\sin\alpha_{neq}\sin i_{eq}\cos C_{seq}\sin\phi_{neq}\cos i_{eq} \\ & \quad +\cos\alpha_{neq}\sin C_{seq}\sin\phi_{neq}\cos i_{eq} \\ & \quad -\cos\phi_{neq}\sin i_{eq}\cos C_{seq}\cos i_{eq}\cos\alpha_{neq} \\ & \quad -\sin\phi_{neq}\sin C_{seq}\cos i_{eq}\cos\alpha_{neq} \\ & \quad +\sin i_{eq}\cos\phi_{neq}\cos\alpha_{neq}\cos C_{seq}\cos i_{eq} \\ & \quad +\sin i_{eq}\sin\phi_{neq}\sin\alpha_{neq}\cos C_{seq}\cos i_{eq}\} \\ & +F_y \times \{\sin\alpha_{neq}\cos i_{eq}\sin\phi_{neq}\cos i_{eq} \\ & \quad +\cos\phi_{neq}\cos i_{eq}\cos i_{eq}\cos\alpha_{neq} \\ & \quad +\sin i_{eq}\sin i_{eq}\cos\phi_{neq}\cos\alpha_{neq} \\ & \quad +\sin i_{eq}\sin i_{eq}\sin\phi_{neq}\sin\alpha_{neq}\} \\ & +F_z \times \{\sin\alpha_{neq}\sin i_{eq}\sin C_{seq}\sin\phi_{neq}\cos i_{eq} \\ & \quad +\cos\alpha_{neq}\cos C_{seq}\sin\phi_{neq}\cos i_{eq} \\ & \quad +\cos\alpha_{neq}\sin i_{eq}\sin C_{seq}\cos i_{eq}\cos\alpha_{neq} \\ & \quad -\sin\phi_{neq}\cos C_{seq}\cos i_{eq}\cos\alpha_{neq} \\ & \quad -\sin i_{eq}\cos\phi_{neq}\cos\alpha_{neq}\sin C_{seq}\cos i_{eq} \\ & \quad -\sin i_{eq}\sin\phi_{neq}\sin\alpha_{neq}\sin C_{seq}\cos i_{eq}\} \end{aligned} \right)$$

$$\times \frac{1}{fd\cos(\phi_{neq}-\alpha_{neq})}$$

$$= \frac{F_x \times 0 + F_y \times (\cos\phi_{neq} - \alpha_{neq}) + F_z \times 0}{fd\cos(\phi_{neq}-\alpha_{neq})} = \frac{F_y}{fd}$$

$= \mathbf{u}$